

# One-Way Electromagnetic Waveguide Formed at the Interface between a Plasmonic Metal under a Static Magnetic Field and a Photonic Crystal

Zongfu Yu,<sup>1</sup> Georgios Veronis,<sup>2</sup> Zheng Wang,<sup>3</sup> and Shanhui Fan<sup>2</sup>

<sup>1</sup>Department of Applied Physics, Stanford University, Stanford, California 94305, USA

<sup>2</sup>Department of Electrical Engineering, Stanford University, Stanford, California 94305, USA

<sup>3</sup>Research Laboratory of Electronics, Massachusetts Institute of Technology, Cambridge, Massachusetts 02139, USA

(Received 10 June 2007; revised manuscript received 25 September 2007; published 17 January 2008)

We demonstrate theoretically the existence of one-way electromagnetic modes in a waveguide formed between a semi-infinite photonic crystal structure and a semi-infinite metal region under a static magnetic field. Such a waveguide provides a frequency range where only one propagating direction is allowed. In this frequency range, disorder-induced scattering is completely suppressed. Such a waveguide also modifies the basic properties of waveguide-cavity interaction.

DOI: 10.1103/PhysRevLett.100.023902

PACS numbers: 42.70.Qs, 41.20.Jb

Understanding and controlling the effects of disorders on wave propagation are becoming increasingly important for nanodevices. In general, the effects of disorders are drastically influenced by time-reversal symmetry properties. In reciprocal nanophotonic systems, which include most photonic crystals and plasmonic waveguides, at any given frequency, for each forward propagating mode, there is a corresponding backward mode with identical mode shapes. In the presence of disorders, these two modes, having maximal modal overlap, always scatter into each other, resulting in backreflection. Such backreflection can be particularly worrisome for slow light systems, which are of current interest for optical signal processing applications. As the group velocity  $v_g$  is reduced, the backreflection increases as  $1/v_g^2$ , and in the limit of  $v_g \rightarrow 0$  may dominate over all other loss mechanisms [1,2].

In systems with broken time-reversal symmetry, the effect of disorders can be suppressed with the use of a *one-way* waveguide. Such a waveguide possesses a *one-way frequency range* where only a forward propagating mode is allowed, with neither radiation nor backward modes. For electrons, an example of a one-way waveguide is the edge states in the quantum hall system [3]. For photons, a design has been proposed in [4,5], which relies upon the presence of a degenerate Dirac point in a reciprocal photonic crystal. Breaking time-reversal symmetry lifts the degeneracy at the Dirac point and creates a band gap. An edge state introduced into this gap then behaves as a one-way waveguide. However, in practical systems, the size of this gap is small since the strength of time-reversal symmetry breaking is generally weak. Thus, it is unclear whether the gap itself will survive disorder and provide the protection against scattering. Indeed, no detailed simulations on the effects of disorders are provided in [4,5].

In this Letter we present a different mechanism for creating a one-way waveguide. The waveguide is formed at the interface between a dielectric photonic crystal that is assumed to be reciprocal, and a free-electron plasmonic metal under a static magnetic field along the direction

perpendicular to the plane of propagation [Fig. 1(a)]. We show that such a waveguide is one-way, provided that the surface-plasmon frequency of the metal surface lies within the band gap of the photonic crystal. In such a system, the

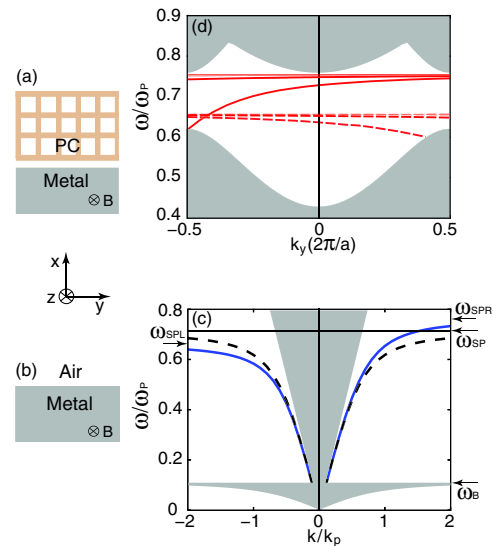


FIG. 1 (color online). (a) A waveguide structure formed at the interface between a photonic crystal (PC) and a free-electron metal subject to an externally applied magnetic field. The metal has a bulk plasmon wavelength  $\lambda_p = \frac{2\pi c}{\omega_p}$ , where  $c$  is the speed of light in vacuum. The photonic crystal consists of a square lattice of dielectric veins ( $\epsilon = 8.9$ ), with a lattice constant  $a = \lambda_p/1.88$ . The thickness of dielectric veins is  $0.2a$ . The distance between the metal and the photonic crystal is  $\lambda_p/3.57$ . (b) Schematics of a metal-air interface, (c) Dispersion relations of surface plasmons at metal-air interfaces in the presence (solid blue line) or absence (dashed black line) of an externally applied static magnetic field. The magnetic field is along the  $z$  direction,  $k_p = \omega_p/c$ . The gray regions represent extended modes in air and metal. (d) Band structure for the waveguide shown in (a). Solid and dashed lines represent modes propagating along positive or negative  $y$  directions, respectively. The gray regions represent extended modes inside the photonic crystal region.

presence of the band gap is intrinsic to the photonic crystal and the metal itself, independent of time-reversal symmetry breaking. Hence the gap can be made very large in size and can survive significant disorders [6]. As a proof of concept, we present direct numerical evidence demonstrating suppression of disorder effects. We also show that the nature of waveguide-cavity interaction, which is at the heart of many integrated devices, can be fundamentally altered.

The design of the structure in Fig. 1(a) relies upon magnetic-field induced nonreciprocity of surface plasmons [7]. In the presence of static magnetic field  $B$  in the  $z$  direction, the dielectric permittivity of the metal is described by a tensor [8]:

$$\vec{\varepsilon}(\omega) = 1 - \frac{\omega_p^2}{(\omega + i/\tau)^2 - \omega_B^2} \times \begin{pmatrix} 1 + i\frac{1}{\tau\omega} & i\frac{\omega_B}{\omega} & 0 \\ -i\frac{\omega_B}{\omega} & 1 + i\frac{1}{\tau\omega} & 0 \\ 0 & 0 & \frac{(\omega + i/\tau)^2 - \omega_B^2}{\omega(\omega + i/\tau)} \end{pmatrix}, \quad (1)$$

where  $\omega_p$  is the bulk plasmon frequency,  $\omega_B = \frac{eB}{m}$  is the cyclotron frequency, decay time  $\tau$  characterizes metal loss,  $e$  is the electron charge, and  $m$  is the electron mass. When the loss is assumed to be infinitesimal, the interface between such a metal and air [Fig. 1(b)] supports surface plasmon with dispersion relation:

$$(\varepsilon_d^2 - \varepsilon_f^2)\sqrt{c^2k_y^2 - \omega^2} + \varepsilon_d\sqrt{c^2k_y^2 - \omega^2\varepsilon_d(1 - \varepsilon_f^2/\varepsilon_d^2)} + \varepsilon_fck_y = 0, \quad (2)$$

where  $\varepsilon_d = 1 - \omega_p^2/(\omega^2 - \omega_B^2)$ ,  $\varepsilon_f = -\omega_p^2\omega_B/(\omega^3 - \omega\omega_B^2)$ , and  $c$  is the speed of light in vacuum. This dispersion relation, with  $\omega_B = 0.1\omega_p$ , is plotted in Fig. 1(c). The linear term of  $k_y$  in Eq. (2) breaks the left-right symmetry of the dispersion relation. In the limit of  $\omega_B \ll \omega_p$ , the frequencies of the left and right propagating modes approach upper limits of  $\omega_{\text{SPL}} = \omega_{\text{SP}} - \frac{\omega_B}{2}$ , and  $\omega_{\text{SPR}} = \omega_{\text{SP}} + \frac{\omega_B}{2}$  at  $k_y \rightarrow \mp\infty$ , respectively, where  $\omega_{\text{SP}} \equiv \frac{\omega_p}{\sqrt{2}}$ . Within the ‘‘one-way’’ frequency range  $\omega_{\text{SPL}} < \omega < \omega_{\text{SPR}}$ , surface plasmon can only propagate in one direction.

The structure as shown in Fig. 1(b) is not an exact one-way waveguide, since radiation modes are always present at any frequency [Fig. 1(c)]. To eliminate radiation modes, we place the metal in close proximity to a photonic crystal consisting of a square array of dielectric veins in air [Fig. 1(a)]. We choose the periodicity  $a$  of the crystal such that the frequency range  $\omega_{\text{SPL}} < \omega < \omega_{\text{SPR}}$  falls within the photonic band gap. Also, we truncate the crystal in such a way without creating any surface mode [9]. The resulting structure is an exact one-way waveguide: In the frequency range  $[0.66\omega_p, 0.76\omega_p]$  there exist modes propagating along the  $+y$  direction but no other modes [Fig. 1(d)]. This range coincides with the one-way range

for the surface plasmons. The lowest band for the right moving modes has substantial bandwidth, and will be used in the following simulations.

We emphasize that one-way waveguide in general does not violate the Bloch theorem. For any periodic system, the Bloch theorem dictates that  $\omega(\frac{\pi}{a}) = \omega(-\frac{\pi}{a})$ , and hence the band structure must be continuous across the Brillouin zone boundary. Most nonreciprocal photonic structures [10–19] have a dispersion relation where the two modes with equal frequencies at Brillouin zone boundaries belong to the same band [Fig. 2(a)]. The continuity of the bands then implies that at any frequency within the band, there are necessarily at least two modes with group velocities  $\frac{d\omega}{dk}$  having opposite signs. These structures [10–19] therefore are not one-way waveguides. In contrast, the dispersion relation of our structure shown in Fig. 2(b) is very different: It satisfies the Bloch theorem since two equal-frequency modes at  $k = \pm\frac{\pi}{a}$  belong to different bands. As a result, the frequency of a band can vary monotonically in the entire Brillouin zone without violating the Bloch theorem.

We numerically investigated the transport properties of our one-way waveguide using the finite-difference frequency-domain method [20,21]. As a direct visualization of the one-way property, in the one-way frequency range a point source in the waveguide radiates only to one direction [Fig. 2(c)]. Moreover, most importantly, such waveguide suppresses disorder-induced backscattering. To simulate the effect of disorders, we place metallic particles in the middle of the waveguide [Fig. 3(a)]. In

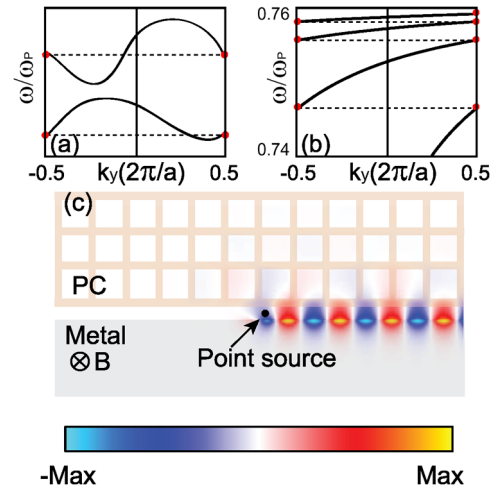


FIG. 2 (color online). (a) Schematic of nonreciprocal dispersion relations that do not have one-way property. (b) A detailed view in the frequency range of  $[0.74\omega_p, 0.76\omega_p]$  of the dispersion relation for the structure shown in Fig. 1(a). In both (a) and (b), the modes at the Brillouin zone edge are highlighted by dots, and dashed lines connect the modes that have the same frequency. (c) Magnetic-field distribution of a propagating wave excited by a dipole source placed in the waveguide structure shown in Fig. 1(a), with a frequency  $\omega = 0.68\omega_p$ .

the absence of external magnetic field ( $\omega_B = 0$ ), the waveguide is reciprocal and these particles cause significant backreflection. Also, as a result of multiple reflections between the particles, the transmission spectra depend sensitively on the numbers and the detailed positions of the particles [dashed lines in Figs. 3(b) and 3(c)]. In contrast, in the presence of an external magnetic field ( $\omega_B = 0.1\omega_P$ ), above  $\omega_{\text{SPL}} = 0.66\omega_P$ , no backreflection is observed [Fig. 3(a)]. The absence of backreflection is independent of the specific properties of the scatterers. For example, we see no observable differences in this frequency range as we vary the number of particles [solid lines in Figs. 3(b) and 3(c)].

The use of a one-way waveguide also fundamentally alters the properties of waveguide-cavity interaction. As an example, we consider the tunneling between two waveguides through a singly degenerate localized resonance [Figs. 4(a) and 4(b)]. The resonance couples to both waveguides to create frequency-selective transfer between the waveguides. In the case of reciprocal waveguides, the resonance decays into both the forward and backward directions [Fig. 4(a)]. Hence at resonance there is always significant reflection, and the transfer occurs to both directions of the output waveguide. On the other hand, with the use of one-way waveguides, the resonator decays only along a single direction into each waveguide [Fig. 4(b)]. Consequently, not only is the reflection fundamentally suppressed, but also at resonance complete transfer occurs to only a single direction of the output waveguide. Hence the structure allows complete channel add or drop filter with a single-mode standing-wave resonator. This is in contrast with all previously considered add or drop filter systems [22–24], including those with magneto-optical

materials [22,23], which all use the equivalent of a rotating state to allow for complete transfer [24].

We confirm the arguments above by numerically simulating the structure shown in Fig. 4(c). Two waveguides are formed in the regions between the metal and the photonic crystal. The crystal region supports a single-mode cavity created by placing an additional dielectric rod ( $\epsilon = 12.25$ ). The cavity has its resonant frequency  $\omega_c$  placed in the one-way frequency range of the waveguides. Additional dielectric scatterers are placed on both sides of the crystal to increase waveguide-cavity coupling. The overall structure has mirror symmetry in both the vertical and horizontal directions, which is important for maximizing transfer efficiency [24].

When external magnetic field is present, at the resonant frequency, complete transfer between the waveguides occurs [Fig. 4(d)]. Also, when the magnetic-field directions between the two metal regions are the same, the two waveguides have opposite propagation directions due to their orientations. Consequently, the transfer occurs only to the backward direction of the output waveguide [Fig. 4(d)]. By reversing the direction of the external magnetic field applied to the upper metal region, the propagation direction of the upper waveguide is reversed, and the wave then transfers completely to the opposite direction [Fig. 4(e)]. The simulations therefore suggest a novel plasmon switch using external magnetic field. In contrast, in the absence of external magnetic field, the structure has significant output to all four ports [Fig. 4(f)].

Up to now we have considered lossless structures, where the modes in the one-way frequency range have real wave vectors  $\beta_f$  in the forward direction and purely imaginary wave vectors  $\beta_b$  in the backward direction. In the presence

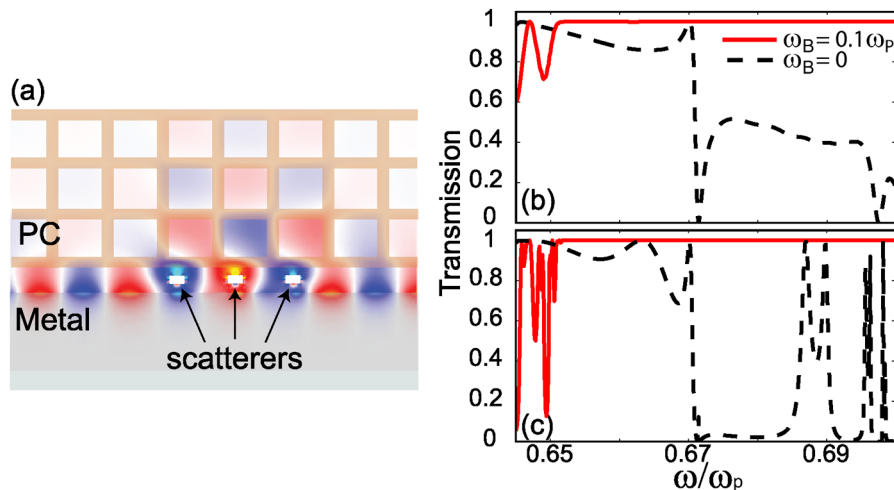


FIG. 3 (color online). (a) Magnetic-field distribution of a propagating wave. Light is incident from the left. The color table is the same as in Fig. 2(c). The waveguide structure is similar to Fig. 1(a) except for the presence of scatterers that consist of metallic particles with a length and width of  $0.11\lambda_P$  and  $0.07\lambda_P$ , respectively. (b),(c) Transmission spectra with one or three particles, respectively. The three-particle structure is shown in (a). The one-particle structure is the same as (a) except that only the middle particle is present. Solid and dashed lines correspond to the cases of  $\omega_B = 0.1\omega_P$  and  $\omega_B = 0$ .

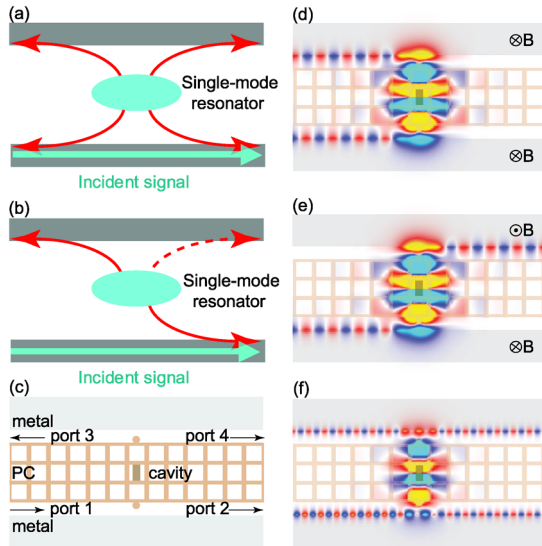


FIG. 4 (color online). (a) Mechanism for resonant coupling between two reciprocal waveguides (gray blocks) through a single-mode resonator (the oval region in the center). The thin arrows indicate the directions of waves that couple out of the resonator into the waveguides. (b) Mechanism for resonant coupling between two one-way waveguides through single-mode resonator. In the lower waveguide, the one-way mode propagates in the forward direction; while in the upper waveguide, the one-way mode propagates either in forward (dashed line) or in the backward (solid line) direction. (c) Simulated structure. The photonic crystal has a lattice constant  $a = \lambda_p/1.81$ . The distance between metal and PC is  $\lambda_p/2.65$ . The cavity has a fundamental resonance mode with frequency  $\omega_0 = 0.6937\omega_p$ . (d)–(f) Magnetic-field distributions at  $\omega_0$  for the structure shown in (c). The color tables are the same as in Fig. 2(c). (d) External magnetic fields with the same direction are applied to both metal regions, (e) External magnetic fields with opposite directions are applied to both metal regions. (f) No externally applied magnetic field.

of loss, both  $\beta_f$  and  $\beta_b$  become complex. However, for a realistic loss parameter of  $\frac{1}{\tau} = 0.01\omega_p$ , which is appropriate for gold, the forward modes are significantly underdamped, i.e.,  $\text{Re}(\beta_f) \gg \text{Im}(\beta_f)$ , while the backward modes are strongly overdamped, i.e.,  $\text{Re}(\beta_b) \gg \text{Im}(\beta_b)$ . Numerical simulation reveals that such a waveguide therefore still provides significant backreflection suppression in the presence of disorders, due to large impedance mismatch between forward and backward modes.

In our design, the one-way bandwidth is proportional to the strength of the external magnetic field. Assuming a static field of 1 Tesla, this range has a width of 28 GHz, which is sizable in the optical wavelength range. Moreover, by using metamaterials with an effective plasmon frequency in the GHz range [25], the predicted effects may be observed in microwave frequency ranges using a more modest static magnetic field. Finally, unlike most magneto-optical materials, metals are widely used in standard opto-

electronic chips, considering plasmonic structures for non-reciprocal applications thus may be of practical interests in general.

This work was supported by NSF (Grant No. EPDT-0622212), AFOSR (Grant No. FA9550-04-1-0437), and the DARPA/MARCO Interconnect Focus Center.

- [1] S. Hughes, L. Ramunno, J. F. Young, and J. E. Sipe, *Phys. Rev. Lett.* **94**, 033903 (2005).
- [2] S. G. Johnson, M. L. Povinelli, M. Soljacic, A. Karalis, S. Jacobs, and J. D. Joannopoulos, *Appl. Phys. B* **81**, 283 (2005).
- [3] S. Datta, *Electronic Transport in Mesoscopic Systems* (Cambridge University Press, Cambridge, U.K., 1995), p. 175.
- [4] F. D. M. Haldane and S. Raghu, arXiv:cond-mat/0503588.
- [5] S. Raghu and F. D. M. Haldane, arXiv:cond-mat/0602501.
- [6] S. Fan, P. R. Villeneuve, and J. D. Joannopoulos, *J. Appl. Phys.* **78**, 1415 (1995).
- [7] R. E. Camley, *Surf. Sci. Rep.* **7**, 103 (1987).
- [8] J. D. Jackson, *Classical Electrodynamics* (Wiley, New York, 1999), 3rd ed., p. 316.
- [9] J. D. Joannopoulos, R. D. Meade, and J. N. Winn, *Photonic Crystals* (Princeton University Press, Princeton, 1995), p. 54.
- [10] A. Figotin and I. Vitebsky, *Phys. Rev. E* **63**, 066609 (2001).
- [11] Z. Yu, Z. Wang, and S. Fan, *Appl. Phys. Lett.* **90**, 121133 (2007).
- [12] K. Y. Jung, B. Donderici, and F. L. Teixeira, *Phys. Rev. B* **74**, 165207 (2006).
- [13] A. M. Merzlikin, A. P. Vinogradov, M. Inoue, and A. B. Granovsky, *Phys. Rev. E* **72**, 046603 (2005).
- [14] A. B. Khanikaev, A. V. Baryshev, M. Inoue, A. B. Granovsky, and A. P. Vinogradov, *Phys. Rev. B* **72**, 035123 (2005).
- [15] I. Bitá and E. L. Thomas, *J. Opt. Soc. Am. B* **22**, 1199 (2005).
- [16] N. Kono and M. Koshiba, *Opt. Express* **13**, 9155 (2005).
- [17] R. L. Espinola, T. Izuhara, M. C. Tsai, and R. M. Osgood, *Opt. Lett.* **29**, 941 (2004).
- [18] M. Levy, *IEEE J. Sel. Top. Quantum Electron.* **8**, 1300 (2002).
- [19] D. M. Pozar, *Microwave Engineering* (John Wiley & Sons, New York, 1998), 2nd ed., p. 497.
- [20] S. D. Wu and E. N. Glytsis, *J. Opt. Soc. Am. A* **19**, 2018 (2002).
- [21] G. Veronis, R. W. Dutton, and S. Fan, *Opt. Lett.* **29**, 2288 (2004).
- [22] Z. Wang and S. Fan, *Photon. Nanostr. Fundam. Appl.* **4**, 132 (2006).
- [23] N. Kono, K. Kakihara, K. Saitoh, and M. Koshiba, *Opt. Express* **15**, 7737 (2007).
- [24] S. Fan, P. R. Villeneuve, J. D. Joannopoulos, and H. A. Haus, *Phys. Rev. Lett.* **80**, 960 (1998).
- [25] J. B. Pendry, A. J. Holden, W. J. Stewart, and I. Youngs, *Phys. Rev. Lett.* **76**, 4773 (1996).